Talanta 148 (2016) 444–453

Contents lists available at ScienceDirect

Talanta

journal homepage: www.elsevier.com/locate/talanta

Determination of high-molecular weight polycyclic aromatic hydrocarbons in high performance liquid chromatography fractions of coal tar standard reference material 1597a via solid-phase nanoextraction and laser-excited time-resolved Shpol'skii spectroscopy

Walter B. Wilson [1], Bassam Alfarhani, Anthony F.T. Moore, Cristina Bisson, Stephen A. Wise [1], Andres D. Campiglia *

Department of Chemistry, University of Central Florida, 4000 Central Florida Blvd, Physical Sciences Room 255, Orlando, FL 32816-2366, United States

ARTICLE INFO

Article history:
Received 26 August 2015
Received in revised form
4 November 2015
Accepted 5 November 2015
Available online 10 November 2015

Keywords:
Polycyclic aromatic hydrocarbons
Solid-phase nanoextraction
Shpol'skii spectroscopy
Gold nanoparticles
Coal tar
Standard reference material 1597a

ABSTRACT

This article presents an alternative approach for the analysis of high molecular weight – polycyclic aromatic hydrocarbons (HMW-PAHs) with molecular mass 302 Da in complex environmental samples. This is not a trivial task due to the large number of molecular mass 302 Da isomers with very similar chromatographic elution times and similar, possibly even virtually identical, mass fragmentation patterns. The method presented here is based on 4.2 K laser-excited time-resolved Shpol'skii spectroscopy, a high resolution spectroscopic technique with the appropriate selectivity for the unambiguous determination of PAHs with the same molecular mass. The potential of this approach is demonstrated here with the analysis of a coal tar standard reference material (SRM) 1597a. Liquid chromatography fractions were submitted to the spectroscopic analysis of five targeted isomers, namely dibenzo[*a,l*]pyrene, dibenzo[*a,e*]pyrene, dibenzo[*a,i*]pyrene, naphtho[*2,3-a*]pyrene and dibenzo[*a,h*]pyrene. Prior to analyte determination, the liquid chromatographic fractions were pre-concentrated with gold nanoparticles. Complete analysis was possible with microliters of chromatographic fractions and organic solvents. The limits of detection varied from 0.05 (dibenzo[*a,l*]pyrene) to 0.24 $\mu g\ L^{-1}$ (dibenzo[*a,e*]pyrene). The excellent analytical figures of merit associated to its non-destructive nature, which provides ample opportunity for further analysis with other instrumental methods, makes this approach an attractive alternative for the determination of PAH isomers in complex environmental samples.

1. Introduction

Standard reference material (SRM) 1597 is a natural complex sample from Coal Tar originally issued by the National Institute of Standards and Technology (NIST) in 1987 [1]. The original Certificate of Analysis for SRM 1597 included 12 certified concentrations of polycyclic aromatic hydrocarbons (PAHs) along with 18 non-certified (reference) concentrations that included PAHs and other polycyclic aromatic compounds. Information on the certified concentrations was obtained with combination of gas chromatography with flame ionization detection (GC/FID) and reversed-phase high-performance liquid chromatography with fluorescence detection (HPLC-FL). Noncertified concentrations assignments were solely based on GC/FID.

Since then, SRM 1597 has found widespread and continued use within the analytical community for the validation of methods in environmental matrices. In addition to the compounds originally included in the Certificate of Analysis, this SRM has been applied to develop methods for the determination of polycyclic aromatic sulfur heterocycles (PASHs) [2,3], PAHs of molecular mass (MM) 278 Da, 300 Da, and 302 Da [1,4,5], methyl substituted benzo[*a*]pyrene isomers [6], other methyl and dimethyl-substituted PAHs [7], stable carbon isotope values and radiocarbon content of individual PAH [8], and to investigate the effects of complex PAH mixtures on the activation of carcinogenic PAHs to DNA-binding derivatives and carcinogenesis [9–11].

To address the need for updating the original certified values and expanding the number of PAHs with assigned values, NIST re-analyzed SRM 1597 and reissued it as SRM 1597a [12]. The Certificate of Analysis for SRM 1597 a included certified concentrations for 34 PAHs and reference values for an additional 36 PAHs and 10 PASHs. PAH concentrations were assigned based on results from gas

* Corresponding author.
E-mail address: andres.campiglia@ucf.edu (A.D. Campiglia).
[1] Present Address: Chemical Sciences Division, Material Measurement Laboratory, National Institute of Standards and Technology, Gaithersburg, Maryland 20899.

http://dx.doi.org/10.1016/j.talanta.2015.11.018
0039-9140/

chromatography/mass spectrometry (GC/MS) and reversed-phase LC-FL. PASHs concentrations were determined based on GC/MS and GC with atomic emission detection (GC/AED) [2].

This article deals with the determination of PAH isomers with MM 302 Da in SRM 1597a. A significant portion of the biological activity of PAH – contaminated samples is now attributed to the presence of high molecular weight – PAHs (HMW-PAHs), i.e. PAHs with MM greater than 300 Da. A crucially relevant toxicological example is dibenzo[*a*,*l*]pyrene (DB[*a*,*l*]P), the most potent carcinogenic PAH known to date [13–15]. Its toxicity is considerably higher than that of benzo[*a*]pyrene, which is the most carcinogenic PAH in the priority pollutants list of the Environmental Protection Agency. There are several more dibenzopyrene isomers that are also carcinogenic, but not to the extent of DB[*a*,*l*]P. Since the carcinogenic properties of HMW-PAHs differ significantly from isomer to isomer, it is important to determine the most toxic isomers even if they are present at much lower concentrations than less toxic isomers. This is not a trivial task since many isomers have very similar chromatographic behaviors and similar, possibly even virtually identical, mass fragmentation patterns.

NIST has identified a total of 23 HMW-PAHs with a MM 302 in SRM 1597a [12]. The assignment of mass fraction values for 17 of these HMW-PAHs was based on the analytical approach shown in Fig. 1. In methods I – III, the coal tar sample was fractionated by normal phase-LC (NPLC) using a semi-preparative aminopropylsilane (NH_2) column that isolated isomeric fractions prior to PAH determination via HPLC-FL or GC/MS. HPLC separation was carried out on a octadecyl (C_{18}) stationary phase. GC separation was accomplished with fused silica capillary columns with one of two stationary phases, namely dimethyl 50% liquid crystalline polysiloxane phase (LC-50) or 50% phenyl-substituted methylpolysiloxane (DB-17 ms). DB-17 ms was also used as the stationary phase in GC/MS methods IV and V to attempt isomers determination without previous sample fractionation.

Previous studies have shown alternative approaches for analyzing PAHs in environmental samples combing liquid chromatography and low resolution multi-wavelength fluorescence detection through the use of chemometric algorithms [16,17]. The approach we present here is based on Shpol'skii spectroscopy, a photoluminescence technique long recognized for its capability in providing efficient and adequate resolution of structural isomers at the concentration ratios found in environmental samples without the aid of chemometrics [18,19]. Its capability results from the unmatched resolution observed from excitation and emission (fluorescence and/or phosphorescence) spectra in Shpol'skii matrixes. The term Shpol'skii matrix refers to a dilute solution of a guest molecule (PAH) in a solvent host (usually an n-alkane) where the solvent freezes to 77 K or below into an ordered polycrystalline matrix. If the dimensions of the PAH and solvent match up well enough, PAH molecules occupy a small number of crystallographic sites (ideally just one) in the host matrix. Matrix isolation of guest molecules reduces inhomogeneous band broadening. The combination of reduced thermal and inhomogeneous broadening produces vibrationally resolved spectra with sharp line widths.

The complications of traditional methodology for 4.2 K measurements are here avoided by using a bifurcated fiber optic probe (FOP) that delivers the excitation light directly into the frozen matrix [20–26]. This approach retains the simplicity of immersing the sample into the liquid cryogen for fast and reproducible freezing, eliminating all the interfaces that could scatter exciting light into the detection system. Frozen samples are prepared in a matter of seconds. The unambiguous determination of targeted PAHs is accomplished via collection of 4.2 K wavelength-time matrices (WTMs). These data formats take advantage of the full dimensionality of fluorescence spectroscopy by combining spectral and lifetime information. Adding the temporal dimension to Shpol'skii spectra provides a particularly selective tool for the determination of structural isomers of MM 302 Da [23–26].

DB[*a*,*l*]P, dibenzo[*a*,*e*]pyrene (DB[*a*,*e*]P), dibenzo[*a*,*i*]pyrene (DB[*a*,*i*]P), dibenzo[*a*,*h*]pyrene (DB[*a*,*h*]P) and naphtho[*2*,*3*-*a*]pyrene (N[*2*,*3*-*a*]P) were selected to demonstrate the potential of laser-excited time-resolved Shpol'skii spectroscopy (LETRSS) for the analysis of dibenzopyrenes in HPLC fractions of SRM 1597 a extracts. The advantages of using solid-phase nanoextraction (SPNE) [25–32] for HPLC-fraction pre-concentration are supported with excellent analytical figures of merit. The accuracy of HPLC-SPNE-LETRSS is demonstrated with statistically equivalent concentrations compared to NIST certified values.

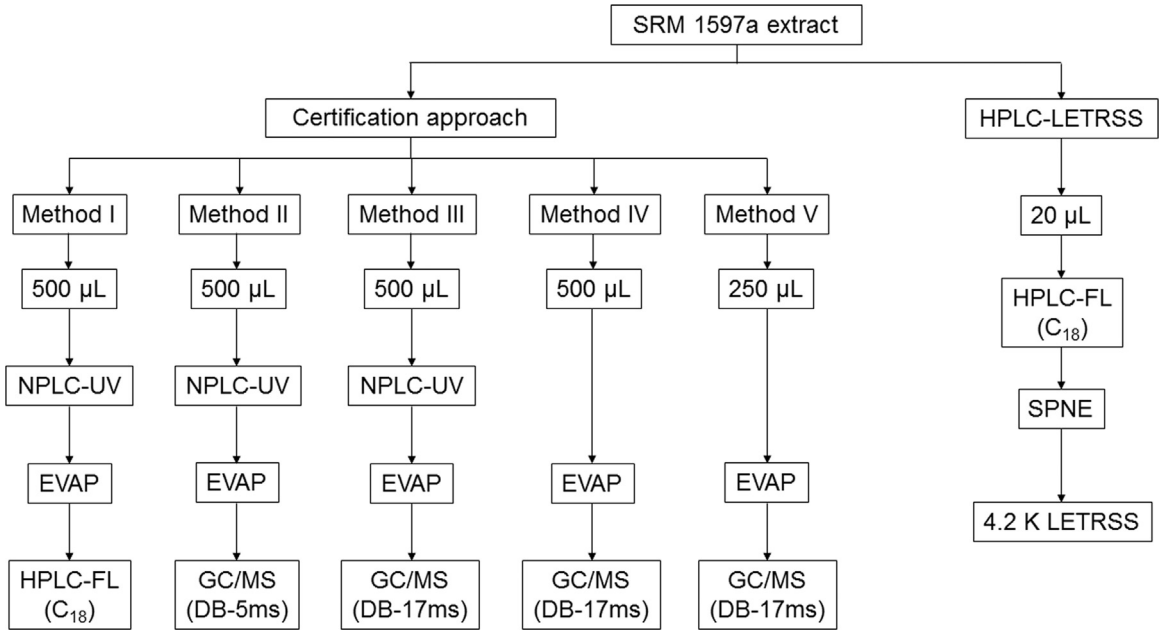

Fig. 1. Schematic diagram of the 5 analytical methods listed in the certificate of analysis of SRM1597a for determining the mass fraction values for HMW-PAHs.

2. Experimental

2.1. Chemicals and reagents

Nanopure water from a Barnstead Nanopure Infinity water system was used throughout. 20 nm average diameter gold nanoparticles (Au NPs) in aqueous solutions (7×10^{11} particles mL^{-1}) were purchased from Ted Pella, Inc. (Redding, CA). HPLC grade methanol and acetonitrile were purchased from Fisher Scientific (Pittsburg, PA). Analytical grade 1-pentanethiol, toluene, n-octane, n-nonane and n-decane were purchased from Acros Organics (Atlanta, GA). DB[*a,l*]P, DB[*a,e*]P, DB[*a,h*]P and DB[*a,i*]P were purchased from Accustandard at their highest available purity (100%). N[*2,3-a*]P was acquired from Sigma-Aldrich (Milwaukee, WI) at 98% purity. The SRM 1597a extract was prepared by NIST (Gaithersburg, MD) according to an experimental procedure reported previously [33]. Briefly, 36 g of the coal tar sample were processed through an open LC column containing attapulgus clay to remove the highly polar constituents in the sample. The column was eluted with approximately 7 L of 10% methylene chloride in n-pentane and the eluent was collected, evaporated and re-dissolved in 4.5 L of toluene. These quantity values were found to extract a large fraction of PAHs from the original coal tar sample.

Note. use extreme caution when handling PAHs that are known to be extremely toxic.

2.2. Pre-concentration of HPLC fractions

HPLC fractions were pre-concentrated via evaporation (EVAP) and SPNE. The SPNE procedure has been described in detail previously [25–32]. Briefly, aliquots of HPLC fractions were mixed with 1 mL of 20 nm Au NPs. The mixture was shaken for 5 min at 1400 rpm and centrifuged for 10 min at 13400 rpm. The supernatant was separated from the precipitate with a micro-pipette. 2 μL of 1-pentanethiol, 48 μL of methanol, and 50 μL of n-alkane (n-octane, n-nonane, or n-decane) were added to the precipitate. The new mixture was shaken for 5 min at 1400 rpm. The n-alkane was removed with a micro-pipette and analyzed via 4.2 K LETRSS. The EVAP procedure involved drying the HPLC fractions under a gentle stream of ultra-high pure nitrogen and then re-dissolving them in 400 μL of n-alkane for 4.2 K LETRSS analysis.

2.3. Ultraviolet–visible absorption spectroscopy

Absorbance spectra were recorded with a single-beam spectrophotometer (model Cary 50, Varian) equipped with a 75 W pulsed xenon lamp, 2 nm fixed bandpass, ±0.1 nm wavelength precision, and 24 000 nm min^{-1} maximum scan rate. All solution measurements were made with a 600 μL quartz cuvette with a 1 cm path length.

2.4. Room temperature fluorescence (RTF) spectroscopy

Steady-state excitation and fluorescence spectra were acquired with a commercial spectrofluorimeter (Photon Technology International). The excitation source was a continuous wave 75-W xenon lamp with broadband illumination from 200 to 2000 nm. The excitation and emission monochromators had the same reciprocal linear dispersion (4 nm mm^{-1}), accuracy (±1 nm), reproducibility (±2 nm) and spectral resolution (0.25 nm). Both gratings had 1200 grooves/nm and were blazed at 300 nm (excitation) and 400 nm (emission). Detection was made with a photomultiplier tube (model 1527) with spectral response from 185 to 650 nm. Instrument control was carried out with commercial software (Felix32) specifically designed for the system. Excitation and emission spectra were corrected for wavelength dependence of excitation light source and detector sensitivity, respectively. Correction was made in the post-acquisition mode using the radiometric correction factors included in Felix32 software. Long pass filters were used when necessary to eliminate second-order emission from the excitation source. Room-temperature measurements were made from un-degassed solutions in 600 μL quartz cuvettes with 1 cm optical path length. 77 K measurements followed the classical procedure of immersing an un-degassed sample solution in a quartz tube into a nitrogen-filled Dewar flask. The length of the quartz tube (25 m) and the design of the Dewar allow for samples to be analyzed without any interference from condensation. Condensation occurs at the top of the Dewar but the sample is analyzed at the bottom section of the quartz tube. A 90° excitation/emission configuration was used in all measurements.

2.5. HPLC Instrumentation

HPLC analysis was performed using a computer-controlled Hitachi (San Jose, CA) HPLC system equipped with a (model L-7100) gradient pump, an (L-7400 UV) detector, and (L-7485) fluorescence detector, an online degasser (L-761) and a (D-7000) control interface. Separation was carried out on a Supelco (Bellefonte, PA) Supelcosil TM LC-PAH column with the following characteristics: 15 cm length, 4 mm diameter, and 5 μm average particle diameters. All sample injections were held constant at 20 μL using a fixed-volume injection loop. HPLC fractions were collected in 7.0 mL amber sample vials with the aid of a Gilson fraction collector (model FC 20313).

2.6. Instrumentation for 4.2 K LETRSS

Measurements were carried out with a multidimensional luminescence system built in our lab. Its complete description and full measuring capabilities – i.e. for absorption, excitation, fluorescence and phosphorescence measurements – have been reported previously [20]. The system was operated in the external trigger mode. Data acquisition parameters (gate delay and gate width) were entered on the control computer with Andor software and the appropriate control signals were sent via a GPIB interface to the pulse generator. Once triggered by the laser, the pulse generator used this information to determine when the image intensifier in the detector head was gated on (gate delay) and for how long it was gated on (gate width). When the intensifier was gated off, the acquired data were transferred from the detector head to the controller card (32-bit Intelligent Bus-Mastering PCI card) in the computer. Complete instrument control was carried out with LabView (National Instruments, version 6.0) based software developed in our lab.

Fluorescence spectra were recorded using a minimum delay of 10 ns, which was sufficient to avoid the need to consider convolution of the laser pulse with the analytical signal. The measuring gate was optimized to collect most of PAH fluorescence and still avoid instrumental noise. Unless otherwise noticed, each spectrum corresponds to the accumulation of 100 laser pulses. The limiting resolution for recording excitation spectra was dictated by the minimum scanning rate of the tunable dye laser, namely 0.1 nm/data point. The best resolution for recording fluorescence spectra was dictated by the limiting resolution of the spectrograph/ICCD system, which corresponded to 0.32–0.40 nm [20].

Fluorescence lifetimes were measured via the WTM procedure, [20] which consists on the three following steps: (1) full sample and background WTM collection; (2) background decay curve subtraction from the fluorescence decay curve at a wavelength of maximum emission for each PAH; and (3) fitting of the background corrected data to single-exponential decays. In cases of

unknown sample composition where the formulation of a correct blank for lifetime background correction was not possible, the fluorescence decay at the base of the target peak was used for background subtraction at the target wavelength. The accuracy of this procedure has been confirmed previously [34] Origin software (version 7.5, Micronal Software, Inc.) was used for curve fitting of fluorescence decays. Fluorescence lifetimes were obtained from decay curves fitted to Eq. (1) with x_0 and y_0 set to a value of zero.

$$y=y_0+A_1e^{[-(x-x_0)t_1]} \quad (1)$$

2.7. Sample freezing procedures

4.2 K fluorescence measurements were carried out with the aid of a cryogenic fiber optic probe [21]. The probe consisted of one delivery and six collection fibers. All fibers were 3 m-long and 500-μm-core-diameter, silica-clad silica with polyimide buffer coating (Poly-micro Technologies, Inc.). The fibers were fed into a 1.2-m-long section of copper tubing that provided mechanical support for lowering the probe into the liquid helium. At the sample end, the fibers were arranged in a conventional six-around-one configuration with the delivery fiber in the center, bundled with vacuum epoxy (Torr-Seal, Varian Products), fed into a metal sleeve, and aligned with the entrance slit of the spectrometer. The dimensions of the sample vial were the following: 30 mm length, 5.5 mm inner diameter, and 7 mm outer diameter. Its maximum volume capacity was 750 μL. The measurement procedure was as follows: after transferring a known volume (typically 50–100 μL) of un-degassed sample solution with a pipette into the sample vial of the cryogenic probe, the tip of the fiber-optic bundle was positioned and held constant with the screw cap above the solution surface. Sample freezing was accomplished by lowering the copper tubing into the liquid helium, which was held in a Dewar with 60 L storage capacity. The liquid helium would typically last three weeks of daily use, averaging 15–20 samples per day. Complete sample freezing took less than 90 s per sample. Replacing the frozen sample involved removing the sample vial from the cryogen container and melting the frozen sample with a heat gun. Because no physical contact between the tip of the fiber-optic bundle and the sample ever occurred during measurements, probe clean up between measurements was not necessary. The entire freeze, thaw, and sample replacement cycle took no longer than 5 min.

3. Results and discussion

3.1. HPLC analysis of SRM 1597a for HMW-PAHs

Previous work reported by Wise et al. demonstrated the ability to separate 12 isomers of MM 302 Da from an SRM 1597 extract using a polymeric C_{18} column [1]. Separation was achieved using a 100% acetonitrile mobile phase, a flow rate of 1.5 mL min^{-1} and a column temperature of 29 °C. Fig. 2A shows a typical fluorescence chromatogram of a standard mixture of DB[*a,l*]P, DB[*a,e*]P, DB[*a,i*]P, N[*2,3-a*]P and DB[*a,h*]P in toluene recorded in our lab. With the exception of the 29 °C column temperature, which we had no instrumental capability to reproduce, the chromatographic conditions were the same as those reported previously [1]. At room temperature, the separation of the five isomers was achieved in 40 min of analysis time. Fluorescence detection using the following time-programmed excitation/emission wavelengths: 0.0 min, 316/424; 10.0 min, 303/398; 20.0 min, 394/434; 29.3 min, 332/460; and 33.0 min, 313/447. All excitation and emission wavelengths corresponded to the maximum values obtained from pure

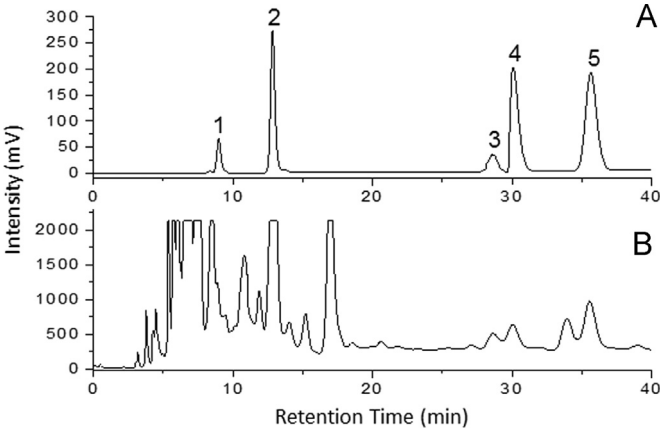

Fig. 2. (A) Fluorescence chromatogram of a synthetic mixture containing (1) DB[*a,l*]P at 19.4 μg L^{-1}, (2) DB[*a,e*]P at 157.3 μg L^{-1}, (3) DB[*a,i*]P at 67.0 μg L^{-1}, (4) N[*2,3-a*]P at 74.3 μg L^{-1} and (5) DB[*a,h*]P at 44.5 μg L^{-1}. These concentrations match the certified concentrations reported for the HMW-PAHs in the certificate of analysis for SRM 1597 a. The mobile phase was 100% acetonitrile and a flow rate of 1.5 mL min^{-1}. Excitation and emission wavelengths were as follows: 316/424 nm (DB[*a,l*]P), 303/398 nm (DB[*a,e*]P), 332/465 nm (DB[*a,i*]P and N[*2,3-a*]P), and 313/447 nm (DB[*a,h*]P). (B) Fluorescence chromatogram of the SRM 1597 a using the same conditions in Fig. 2A.

standard spectra in 100% acetonitrile (data not shown). Three chromatographic runs of the same standard mixture recorded from three independent injections of 20 μL aliquots provided the following average retention times (min): 8.89 ± 0.02 (DB[*a,l*]P), 12.8 ± 0.06 (DB[*a,e*]P), 28.5 ± 0.23 (DB[*a,i*]P), 30.0 ± 0.25 (N[*2,3-a*]P) and 35.6 ± 0.29 (DB[*a,h*]P). Fig. 2B shows the fluorescence chromatogram of the SRM 1597 a sample diluted with toluene to a ratio that provided concentrations of DB[*a,l*]P (19.5 μg L^{-1}), DB[*a,e*]P (157.3 μg L^{-1}), DB[*a,i*]P (67.0 μg L^{-1}), N[*2,3-a*]P (74.3 μg L^{-1}) and DB[*a,h*]P (44.5 μg L^{-1}) identical to those from the pure standards. The complexity of the coal tar sample can be clearly noticed by the large number of chromatographic peaks. Comparison of fluorescence intensities to those in Fig. 2A, suggest potential overlapping of co-eluted peaks that could result in the inaccurate determination of the targeted isomers via HPLC analysis.

3.2. 4.2 K LETRSS analytical figures of merit

Fig. 3 shows the molecular structures of the 23 isomers with molecular mass of 302 Da previously identified by NIST in the SRM 1597 a. For the specific case of the 5 targeted isomers, the host-guest molecular length matching criterion for best spectral resolution [29,34] leads to one of the following three n-alkanes: n-octane (DB[*a,l*]P and DB[*a,e*]P), n-nonane (DB[*a,i*]P), and n-decane (N[*2,3-a*]P and DB[*a,h*]P). As shown in Figs. S1–S5, these three solvents provide excitation and fluorescence spectra with vibrational features commonly observed in 77 K Shpol'skii spectroscopy. Sample excitation with the tunable dye laser at the maximum excitation wavelength of each isomer – i.e., 321 nm (DB[*a,l*]P), 307 nm (DB[*a,e*]P), 398 nm (DB[*a,i*]P, 336 nm (N[*2,3-a*]P) and 314 nm (DB[*a,h*]P) – would require the use of three laser dyes, namely Rhodamine 640 (DB[*a,e*]P and DB[*a,h*]P), DCM (DB[*a,l*]P and N[*2,3-a*]P) and LDS 798 (DB[*a,i*]P). For the sake of operational simplicity, we opted to use a single laser dye (DCM) for sample excitation within the 305–325 nm range.

Table 1 lists the excitation wavelengths that provided the highest fluorescence intensity for each HMW-PAH within the wavelength excitation range of DCM. The delay (t_d) and gate (t_g) widths were optimized to collect most of the PAH fluorescence and still avoid instrumental noise. The gate steps (t_s) were optimized to record a sufficient numbers of data points within the

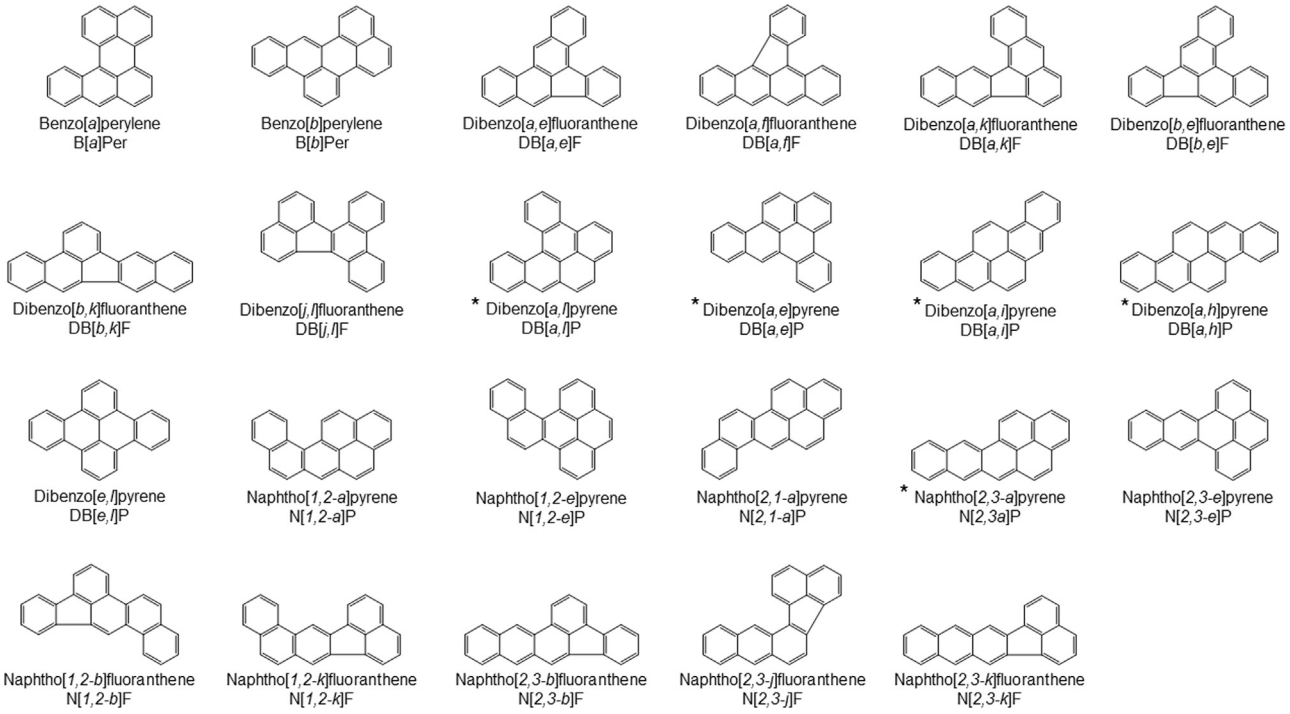

Fig. 3. Molecular structures of the 23 PAH isomers with molecular mass of 302 Da previously identified by NIST in the SRM 1597 a. The isomers determined in this study have asterisk (*).

lifetime decay of each PAH. With the exception of DB[*a,i*]P, the highest fluorescence intensity and narrowest full-width half-maximum (FWHM) were obtained with the n-alkane that best matched the length of the PAH. Within a confidence interval of 95% ($N_1 = N_2 = 3$), [35] the highest fluorescence intensity and narrowest FWHM of DB[*a,i*]P were obtained in n-octane and n-decane. The choice of n-alkane did not cause considerable changes in the lifetimes of the studied PAHs. Well-behaved, single exponential decays of fluorescence intensity versus time were observed in all cases. The first two lifetimes decay agreed to within about 1% and the residuals and showed no systematic trends.

Fig. 4 A–E show the 4.2 K LETRSS fluorescence spectra of DB[*a,l*]P, DB[*a,e*]P, DB[*a,i*]P, N[*2,3-a*]P and DB[*a,h*]P in their best matching n-alkane solvent. Table 2 summarizes the 4.2 K LETRSS analytical figures of merit (AFOMs) of each isomer using the current International Union for Pure and Applied Chemistry (IUPAC) guidelines [36]. Calibration curves were built using a minimum of five standard solutions of each PAH. All fluorescence measurements were made at the maximum emission wavelength of each PAH. No attempts were made to reach the upper concentration limit of the linear dynamic range (LDR). All intensities plotted in the calibration graphs were measured under the optimum delay and gate times for each PAH (Table 1). The existence of linear relationships was confirmed with comparing experimental F-test values (F_{exp}) to

Table 1
Spectral comparison of five HMW-PAH isomers via 4.2 K LETRSS.

HMW-PAH [a]	n-alkane	$\lambda_{ex}/\lambda_{em}$ [b] (nm)	$t_d/t_g/t_s$ [c] (ns)	I_F ($\times 10^5$) [d,g] (counts)	FWHM [e,g] (nm)	τ [f,g] (ns)
DB[*a,l*]P	n-octane	318.0/415.4	10/250/6	39.4 ± 0.81	0.23 ± 0.01	78.1 ± 1.0
	n-nonane	318.0/415.7		7.28 ± 0.17	0.69 ± 0.01	77.5 ± 0.83
	n-decane	318.0/415.6		6.92 ± 0.11	0.52 ± 0.01	77.3 ± 0.86
DB[*a,e*]P	n-octane	306.4/392.2	10/150/5	1.19 ± 0.07	0.28 ± 0.01	54.3 ± 1.4
	n-nonane	305.0/391.9		0.64 ± 0.01	0.38 ± 0.03	63.9 ± 2.5
	n-decane	306.0/392.4		0.72 ± 0.03	0.61 ± 0.03	67.0 ± 1.3
DB[*a,i*]P	n-octane	312.0/428.3	10/650/20	11.6 ± 0.20	0.32 ± 0.01	216.2 ± 1.7
	n-nonane	312.0/428.8		8.57 ± 0.10	0.51 ± 0.01	226.2 ± 2.4
	n-decane	312.0/428.3		11.9 ± 0.30	0.33 ± 0.01	211.6 ± 7.2
N[*2,3-a*]P	n-octane	318.0/456.9	0/25/1	16.5 ± 0.70	0.72 ± 0.05	7.90 ± 0.11
	n-nonane	317.0/455.8		10.2 ± 0.50	1.12 ± 0.09	7.90 ± 0.01
	n-decane	317.0/457.8		26.4 ± 0.30	0.29 ± 0.01	6.83 ± 0.05
DB[*a,h*]P	n-octane	310.0/445.6	0/15/1	17.1 ± 0.10	0.44 ± 0.01	6.17 ± 0.14
	n-nonane	310.0/446.5		31.6 ± 0.60	0.58 ± 0.02	6.30 ± 0.10
	n-decane	310.0/446.6		50.0 ± 0.60	0.31 ± 0.01	6.31 ± 0.09

[a] All HMW-PAH solutions were made in their perspective n-alkane solvents.
[b] Excitation (λ_{exc}) and fluorescence (λ_{em}) wavelengths.
[c] Optimum gate delay (t_d), gate width (t_g) and gate step (t_s).
[d] Fluorescence intensity (I_F) of HMW-PAHs in the frozen n-alkane matrices. All fluorescence intensities represent an average of nine independent measurements made at the maximum emission wavelengths of each HMW-PAH.
[e] Full width at half-maximum (FWHM).
[f] Average fluorescence lifetime of three measurements taken from three frozen aliquots.
[g] The uncertainty listed with each value is an expanded uncertainty about the mean of the results based on the standard deviation obtained from six measurements.

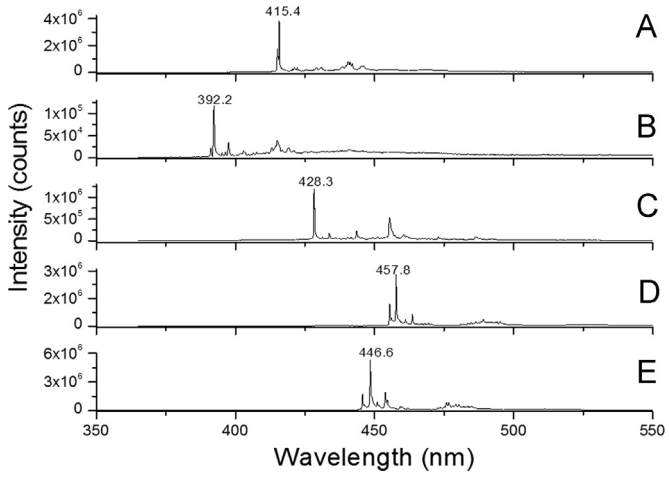

Fig. 4. 4.2 K LETRSS fluorescence spectra of 100 ng mL^{-1} (A) DB[*a,l*]P in n-octane (λ_{exc}=318.0 nm, λ_{em}=415.4 nm, 0 ns delay and 250 ns gate time); (B) DB[*a,e*]P in n-octane (λ_{exc}=306.4 nm, λ_{em}=392.4 nm, 10 ns delay and 150 ns gate time); (C) DB[*a,i*]P in n-decane (λ_{exc}=312.0 nm, λ_{em}=428.3 nm, 10 ns delay and 650 ns gate time); (D) N[*2,3-a*]P in n-decane (λ_{exc}=317.0 nm, λ_{em}=457.8 nm, 0 ns delay and 25 ns gate time) and (E) DB[*a,h*]P in n-decane (λ_{exc}=310.0 nm, λ_{em}=446.6 nm, 0 ns delay and 15 ns gate time). All spectra correspond to the accumulation of 100 laser pulses. The spectrograph slit was 42 μm.

Table 2
AFOM for the five HMW-PAHs via 4.2 K LETRSS in their optimal n-alkane solvents.

HMW-PAH[a]	n-alkane	LDR[b] (μg L^{-1})	F_{exp} [c]	LOD[d] (μg L^{-1})	RSD[e] (%)
DB[*a,l*]P	n-octane	0.06–100	0.01	0.02	4.0
DB[*a,e*]P	n-octane	0.72–100	0.03	0.24	5.9
DB[*a,i*]P	n-decane	0.40–100	0.20	0.13	2.2
N[*2,3-a*]P	n-decane	0.07–50	0.07	0.02	2.2
DB[*a,h*]P	n-decane	0.14–50	0.02	0.04	2.7

[a] All HMW-PAH solutions were made in their perspective n-alkane solvents.
[b] LDR, linear dynamic range; lower concentration limit=limit of quantitation (LOQ).
[c] F_{exp} is the ratio of residual variance to squared pure error, critical F (0.05,16,13)=2.46 is the critical value of F with (I–2)=16 and ($I-L$)=13 degrees of freedom at 95% confidence level, where I is the number of calibration samples (18) and L the number of concentration levels (5).
[d] LOD, limit of detection of HMW-PAHs.
[e] Relative standard deviation (RSD)=S_F/I_Fx100, where S_F is the standard deviation of the average calculated from six fluorescence measurements at medium linear PAH concentrations.

Table 4
Comparison of the certified and the calculated for 5-HMW PAHs.

HMW-PAH	Reported values [a] (mg Kg^{-1})	Experimental [b] (mg Kg^{-1})	t-test [c]
DB[*a,l*]P	1.12 ± 0.08	0.93 ± 0.16	1.50
DB[*a,e*]P	9.08 ± 0.20	9.47 ± 0.51	1.43
DB[*a,i*]P	3.87 ± 0.17	3.64 ± 0.36	1.14
N[*2,3-a*]P	4.29 ± 0.45	3.67 ± 0.79	1.45
DB[*a,h*]P	2.57 ± 0.15	2.50 ± 0.27	0.48

[a] Mass fraction and standard deviations from the certificate of analysis for SRM 1597 a.
[b] Mass fraction and standard deviations determine from the HPLC fractions via 4.2 K LETRSS.
[c] t-test of PAH concentrations from HPLC fractions compared to concentration values listed in the certificate of analysis. $t_{critical}$=2.78 (α=0.05; N_{rep}=2–5 and N_{exp}=3).

critical F-test values (F_{crit}). F_{exp} were calculated using Eq. (2):.

$$F_{exp}=\left(\frac{S_{y/x}}{S_y}\right)^2 \tag{2}$$

where $S_{y/x}$ is the residual standard deviation and S_y is the pure error. These parameters can be calculated from the calibration data with Eqs (3) and (4):

$$S_{y/x}=\sqrt{\frac{\sum_{i=1}^{I}\left(y_i-\hat{y}_l\right)^2}{I-2}} \tag{3}$$

$$S_y=\sqrt{\frac{\sum_{l=1}^{L}\sum_{q=1}^{Q}\left(y_{lq}-y_l\right)^2}{I-Q}} \tag{4}$$

where y_i and $\hat{y}_l$ are the experimental and estimated response values for sample i, y_{lq} is the calibration response for replicate q at level l, y_l is the mean response at level l, and I, L, and Q are the total number of calibration samples, levels, and replicates at each level, respectively. In all cases, the F_{exp} was lower than F_{crit} demonstrating the excellent linear relationships between PAH concentrations and fluorescence signal. The limits of detection were calculated according to Eq. (5):

$$\mathrm{LOD}=\frac{3.3S_{y/x}}{A}\sqrt{1+h_0+\frac{1}{I}} \tag{5}$$

where A to the slope of the calibration graph, I is the number of

Table 3
AFOM comparison for the pre-concentration of the 5 HMW-PAHs in HPLC fractions.

	EVAP-LETRSS					SPNE-LETRSS				
HMW-PAH [a]	OR [b] (%)	LDR [c] (μg L^{-1})	F_{exp} [d]	LOD [e] (μg L^{-1})	RSD [f] (%)	OR [b] (%)	LDR [c] (μg L^{-1})	F_{exp} [d]	LOD [e] (μg L^{-1})	RSD [f] (%)
DB[*a,l*]P	100. ± 3.4	1.1–100	0.28	0.4	3.4	98.2 ± 5.5	0.2–10	0.04	0.05	5.6
DB[*a,e*]P	97.2 ± 4.4	14.–100	0.05	4.6	4.5	99.5 ± 2.8	1.8–10	0.02	0.59	2.8
DB[*a,i*]P	97.5 ± 1.9	7.9–100	0.01	2.6	2.0	102.7 ± 3.2	1.0–10	0.02	0.34	3.1
N[*2,3-a*]P	98.6 ± 2.6	1.4–100	0.28	0.5	2.4	102.6 ± 4.1	0.2–10	0.27	0.06	4.0
DB[*a,h*]P	98.4 ± 2.8	2.8–100	0.01	0.9	2.9	102.2 ± 6.0	0.4–10	0.05	0.12	5.9

[a] All HMW-PAH synthetic mixture solutions were made in methanol with the concentration ranging from 0–100 μg L^{-1} (EVAP) and 0–10 μg L^{-1} (SPNE).
[b] OR, overall recovery of HMW-PAHs calculated with equation 5.
[c] LDR, linear dynamic range; lower concentration limit=limit of quantitation (LOQ).
[d] F_{exp} is the ratio of residual variance to squared pure error, critical F(0.05,16,13)=2.46 is the critical value of F with ($I-2$)=16 and ($I-L$)=13 degrees of freedom at 95% confidence level, where I is the number of calibration samples (18) and L the number of concentration levels (5).
[e] LOD, limit of detection of HMW-PAHs.
[f] Relative standard deviation (RSD)=$S_F/I_F \times 100$, where S_F is the standard deviation of the average calculated from six fluorescence measurements at medium linear PAH concentrations.

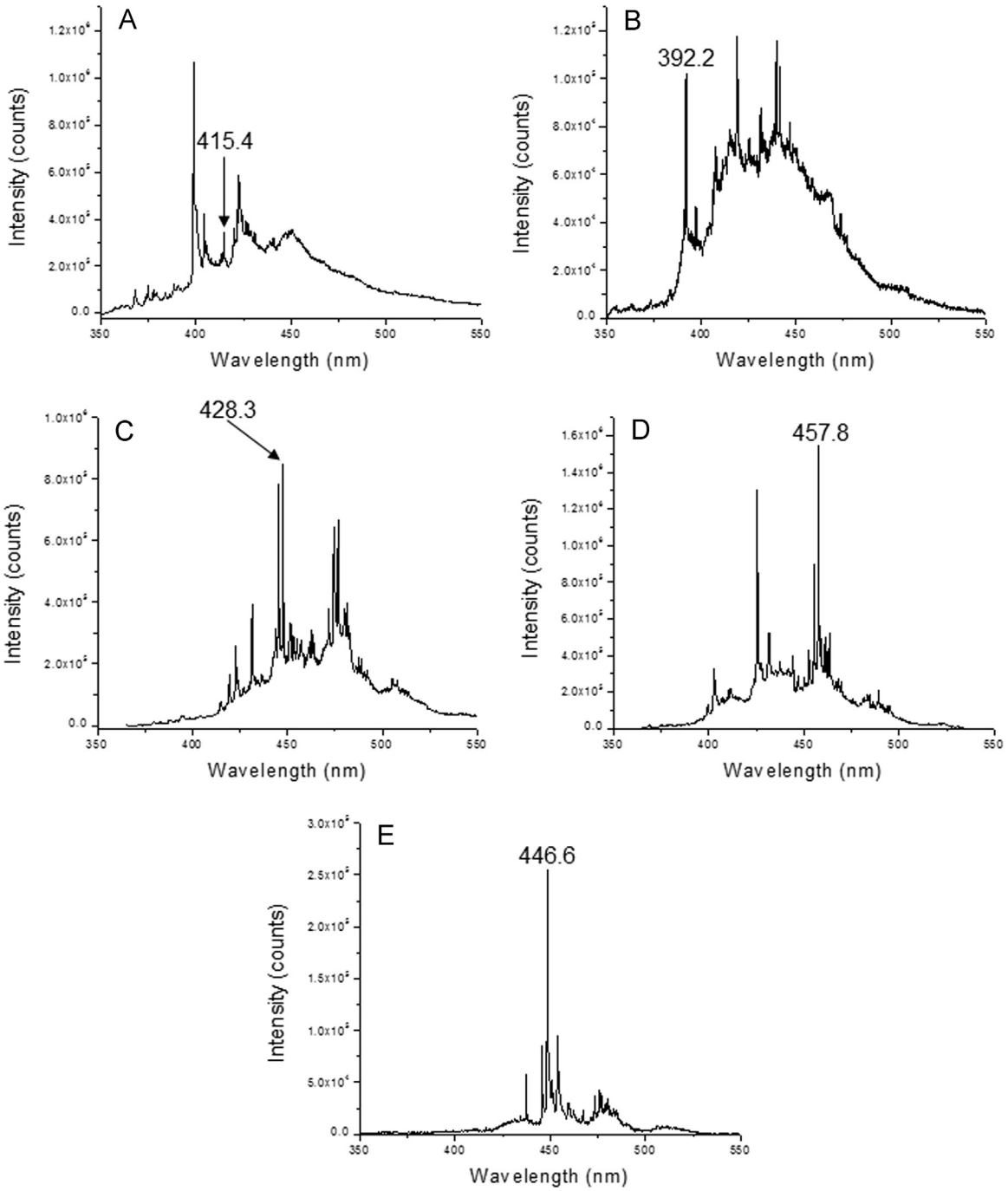

Fig. 5. 4.2 K LETRSS fluorescence spectra of the HPLC fractions obtained from the SRM 1597a. In each spectrum, the target HMW-PAH isomer and experimental parameters were the following: (A) DB[*a,l*]P in n-octane (λ_{exc}=318.0 nm, λ_{em}=415.4 nm, 0 ns delay and 250 ns gate time); (B) DB[*a,e*]P in n-octane (λ_{exc}=306.4 nm, λ_{em}=392.4 nm, 10 ns delay and 150 ns gate time); (C) DB[*a,i*]P in n-decane (λ_{exc}=312.0 nm, λ_{em}=428.3 nm, 10 ns delay and 650 ns gate time); (D) N[*2,3-a*]P in n-decane (λ_{exc}=317.0 nm, λ_{em}=457.8 nm, 0 ns delay and 25 ns gate time) and (E) DB[*a,h*]P in n-decane (λ_{exc}=310.0 nm, λ_{em}=446.6 nm, 0 ns delay and 15 ns gate time). All spectra correspond to the accumulation of 100 laser pulses. The spectrograph slit was 42 μm.

calibration samples, and h_0 is the leverage for the blank sample shown Eq. (6):

$$h_0 = \frac{C_{cal}^2}{\sum_{i=1}^{I}(C_i - C_{cal})^2} \quad (6)$$

where C_{cal} refers to the mean calibration concentration and C_i is each of the calibration concentration values. The LODs varied from 0.02 μg L^{-1} (DB[*a,l*]P and N[*2,3-a*]P) to 0.24 μg L^{-1} (DB[*a,e*]P). Similar concepts apply to the limit of quantitation (LOQ) as shown in Eq. (7),

$$LOQ = \frac{10S_{y/x}}{A}\sqrt{1+h_0+\frac{1}{I}} \quad (7)$$

which corresponds to lowest linear concentration in LDR. The relative standard deviations (RSD) values reflect the excellent reproducibility of LETRSS measurements. All further studies were carried out using the n-alkane solvents listed in Table 2.

3.3. Pre-concentration of HPLC fractions for 4.2 K LETRSS analysis

Several approaches have been reported for the pre-

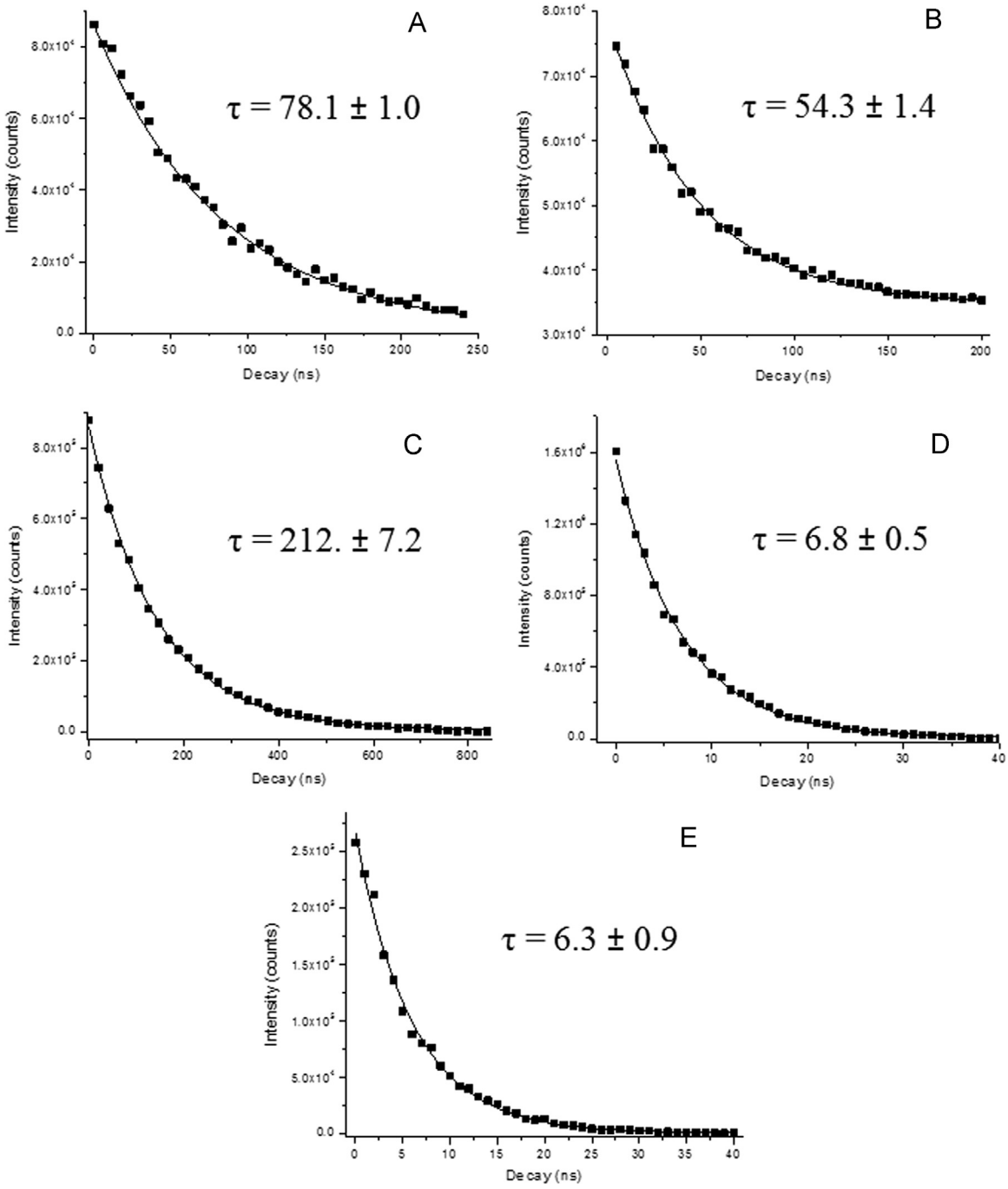

Fig. 6. 4.2 K LETRSS fluorescence lifetimes of the HPLC fractions obtained from the SRM 1597 a. In each lifetime, the target HMW-PAH isomer and experimental parameters were the following: (A) DB[*a,l*]P in n-octane (λ_{exc}=318.0 nm, λ_{em}=415.4 nm, 0 ns delay and 250 ns gate time); (B) DB[*a,e*]P in n-octane (λ_{exc}=306.4 nm, λ_{em}=392.4 nm, 10 ns delay and 150 ns gate time); (C) DB[*a,i*]P in n-decane (λ_{exc}=312.0 nm, λ_{em}=428.3 nm, 10 ns delay and 650 ns gate time); (D) N[*2,3-a*]P in n-decane (λ_{exc}=317.0 nm, λ_{em}=457.8 nm, 0 ns delay and 25 ns gate time) and (E) DB[*a,h*]P in n-decane (λ_{exc}=310.0 nm, λ_{em}=446.6 nm, 0 ns delay and 15 ns gate time). All spectra correspond to the accumulation of 100 laser pulses. The spectrograph slit was 42 μm.

concentration of PAHs from HPLC fractions. These include liquid–liquid extraction (LLE) [24,34,37], solid-phase extraction (SPE) [24,34,37], evaporation (EVAP) [1,33] and SPNE [25]. This article compares the analytical performance of EVAP and SPNE for the LETRSS analysis of the five targeted isomers. Both methods have the strengths of simplicity, cost effectiveness and reduced solvent consumption. Pre-concentration via EVAP is accomplished by applying a steady stream of ultrapure nitrogen gas for approximately 30 min and re-dissolving the solid residue with microliters of Shpol'skii solvent for LETRSS analysis. SPNE pre-concentrates PAHs by mixing the HPLC fraction with gold nanoparticles (Au NPs). After centrifugation and decantation of the supernatant, the Au NPs precipitate is mixed with a PAH releasing solvent mixture (1-pentanethiol/methanol/n-alkane) for LETRSS analysis.

Table 3 summarizes the AFOMs of HPLC-EVAP-LETRSS and HPLC-SPNE-LETRSS analysis for the five HMW-PAHs. Overall recovery (OR) values were calculated according to Eq. (8):

$$OR(\%)=\frac{[PAH]_A * V_A}{C_{PAH} * V_S} * 100 \quad (8)$$

where C_{PAH} refers to the PAH concentration in the original sample, V_S to the extracted volume of sample, $[PAH]_A$ corresponds to the

Table 5
Lifetime (ns) analysis[a] of 5 HMW-PAH isomers.

HMW-PAH	Standard [b,c]	SRM 1597a[c,d]	*t*-test [e]
DB[*a*,l]P	78.1 ± 1.0	80.4 ± 2.7	0.37
DB[*a*,*e*]P	54.3 ± 1.4	51.4 ± 0.6	2.34
DB[*a*,*i*]P	212. ± 7.2	200. ± 5.2	2.29
N[2,3-*a*]P	6.83 ± 0.1	7.13 ± 0.2	2.23
DB[*a*,*h*]P	6.31 ± 0.1	6.14 ± 0.1	0.81

[a] The fluorescence lifetime corresponds to the average of three individual measurements taken from three frozen aliquots at the maximum fluorescence wavelength.
[b] The fluorescence lifetime corresponds to the PAH in a standard solution prepared in its optimum n-alkane solvent.
[c] The uncertainty listed with each value is an expanded uncertainty about the mean of the results based on the standard deviation obtained from six measurements.
[d] The fluorescence lifetime corresponds to the PAH in the HPLC fraction of the coal tar sample in its optimum n-alkane solvent. The uncertainty listed with each value is an expanded uncertainty of the means of the results based on the standard deviation from six measurements.
[e] *t*-test of PAH lifetimes from HPLC fraction compared to standard values. $t_{critical}$=2.78 (α=0.05; N=6).

concentration of PAH in the final volume of n-alkane solvent (V_A). As shown in Fig. S6, the optimum V_A values for EVAP were 400 μL. Previous work in our lab has shown that 50 μL of n-alkane solvent is sufficient to achieve excellent analytical recoveries of PAHs [25–30]. Within a confidence interval of 95% and three replicate trials (α=0.05; N=3), the obtained overall recoveries in Table 3 for both pre-concentration methods were statistically equivalent to 100% [35].

Each calibration curve was built with at least five synthetic mixtures of HMW-PAHs. Each signal plotted in the calibration graph was the average of at least three HPLC-LETRSS measurements recorded from three independent aliquots. AFOM were calculated based on the same equations described in Section 3.2. No efforts were made to reach the upper linear concentration of the LDR. SPNE provided better LODs than EVAP. The LOD improvements result from the 8 × smaller n-alkane volume (V_A) of the procedures of SPNE (50 μL) in comparison to the EVAP (400 μL). All further studies were then carried out using SPNE as the pre-concentrating approach for HPLC-LETRSS analysis.

3.4. Accuracy of HPLC-SPNE-LETRSS

Table 4 compares the NIST mass fraction values of the five targeted HMW-PAHs to those obtained in our lab via HPLC-SPNE-LETRSS. The NIST values correspond to the averages of the mass fractions obtained with methods *I–V* (see Fig. 1). Within a confidence interval of 95% and three replicate trials (N=3), the mass fractions obtained via HPLC-SPNE-LETRSS were statistically equivalent to the reported NIST values. It should be noted that only one of the NIST methods (Method III) was able to determine all five isomers in the coal tar sample extract. Fig. 5A–E shows the 4.2 K fluorescence spectra and Fig. 6A–E shows the lifetimes of the five targeted isomers obtained from the HPLC fractions of the coal tar sample. Each spectrum was recorded using the best gate and excitation wavelengths listed in Table 1.

Table 5 compares the 4.2 K fluorescence lifetimes of pure standards to those recorded from HPLC fractions of the SRM 1597 a sample. The statistical equivalence we observed in all cases (α=0.05; N_1=N_2=6) [35] confirms peak assignments for the unambiguous determination of each molecular mass 302 isomer. Single exponential decays were observed in all cases demonstrating peak purity of HPLC fractions for accurate quantitative analysis of HMW-PAHs.

4. Conclusion

Chemical analysis of PAHs with MM 302 is of great environmental and toxicological importance. Many of them are highly suspect as etiological agents in human cancer. Because their carcinogenic properties differ significantly from isomer to isomer, it is of paramount importance to determine the most toxic isomers even if they are present at much lower concentrations than their less toxic isomers. The main problems that confront HPLC and GC/MS arise from the large number of HMW-PAH isomers with very similar elution times and similar, possibly even virtually identical, mass fragmentation patterns. The approach presented here is based on HPLC-SPNE-LETRSS analysis. The spectral and lifetime information obtained with LETRSS provide the required selectivity for the unambiguous determination of PAH isomers in the HPLC fractions. Prior to LETRSS analysis, HPLC fractions are pre-concentrated via SPNE, an environmentally friendly extraction procedure based on the adsorption of PAHs on the surface of Au NPs [25–30]. Complete SPNE-LETRSS analysis is possible with microliters of HPLC fractions and organic solvent. The excellent analytical figures of merit associated to its non-destructive nature, which provides ample opportunity for further analysis with other instrumental methods makes this approach an attractive alternative for the analysis of isomers of HMW-PAHs in complex environmental samples.

Disclaimer

Certain commercial equipment or materials are identified in this paper to specify adequately the experimental procedure. Such identification does not imply recommendation or endorsement by NIST, nor does it imply that the materials or equipment identified are necessarily the best available for the purpose.

Appendix A. Supplementary material

Supplementary material associated with this article can be found in the online version at http://dx.doi.org/10.1016/j.talanta.2015.11.018.

References

[1] S.A. Wise, B.A. Benner, H. Liu, G.D. Byrd, A. Colmsjoe, Separation and identification polycyclcic aromatic hydrocarbon isomers of molecular weight 302 in complex mixtures, Anal. Chem. 60 (1988) 630–637.
[2] S.G. Mössner, S.A. Wise, Determination of polycyclic aromatic sulfur heterocycles in fossil fuel-related samples, Anal. Chem. 71 (1999) 58–69.
[3] B. Schmid, J.T. Andersson, Critical examination of the quantification of aromatic compounds in three standard reference materials, Anal. Chem. 69 (1997) 3476–3481.
[4] P. Schubert, M.M. Schantz, L.C. Sander, S.A. Wise, Determination of polycyclic aromatic hydrocarbons with molecular weight 300 and 302 in environmental-matrix standard reference materials by gas chromatography/mass spectrometry, Anal. Chem. 75 (2003) 234–246.
[5] S.A. Wise, A. Deissler, L.C. Sander, Liquid chromatographic determination of polcyyclic aromatic hydrocarbon isomers of molecular weight 278 and 302 in environmental standard reference materials, Polycycl. Aromat. Comp. 3 (1993) 169–184.
[6] P. Garrigues, J. Bellocq, S.A. Wise, Determination of metylbenzo[*a*]pyrene isomers in a coal-tar standard reference material using liquid-chromatography and shpol'skii spectrometry, Fresenius' J. Anal. Chem. 336 (1990) 106–110.
[7] D.L. Poster, M.J. Lopez de Alda, S.A. Wise, J.C. Chuang, J.L. Mumford, Determination of PAHs in combustion-related samples and in SRM 1597, complex mixture of PAHs from coal tar, Polycycl. Aromat. Comp. 20 (2000) 79–95.
[8] C.M. Reddy, A. Pearson, L. Xu, A.P. McNichol, B.A. Benner Jr., S.A. Wise, G. A. Klouda, L.A. Crrie, T.I. Eglinton, Radiocarbon as a tool to apportion the sources of polycyclic aromatic hydrocarbons and black carbon in environmental samples, Environ. Sci. Technol. 36 (2002) 1774–1782.
[9] C.P. Marston, C. Pereira, J. Ferguson, K. Fischer, O. Hedstrom, W.M. Dashwood,

W.M. Baird, Effect of a complex environmental mixture from coal tar containing polycyclic aromatic hydrocarbons (PAH) on the tumor initiation, PAH-DNA binding and metabolic activation of carcinogenic PAH in mouse epidermis, Carcinogenesis 22 (2001) 1077–1086.
[10] B. Mahadevan, H. Parsons, T. Musafia, A.K. Sharma, S. Amin, C. Pereira, W. M. Baird, Effect of artifical mixtures of environmental polycyclcic aromatic hydrocarbons present in coal tar, urban dust, and diesel exhaust particulates on MCF-7 cells in culture, Environ. Mol. Mutagen. 44 (2004) 99–107.
[11] B. Mahadevan, C.P. Marston, W.M. Dashwood, Y.H. Li, C. Pereira, W.M. Baird, Effect of a standardized complex misture derived from coal tar on the metabolic activation of carcinogenic polycyclic aromatic hydrocarbons in human cells in culture, Chem. Res. Toxicol. 18 (2005) 224–231.
[12] S.A. Wise, D.L. Poster, S.D. Leigh, C.A. Rimmer, S. Mössner, P. Schubert, L. C. Sander, M.M. Schantz, Polycyclic aromatic hydrocarbons (PAHs) in a coal tar standard reference material – SRM 1597a updated, Anal. Bioanal. Chem. 398 (2010) 717–728.
[13] E.L. Cavalieri, S. Higginbotham, N.V.S. RamaKrishna, P.D. Devanesan, R. Todorovic, E.G. Rogan, S. Salmasi, Comparative dose-response tumorigenicity studies of dibenzo[a,l]pyrene versus 7,12-dimethylbenz[a]anthracene, benzo[a]pyrene and 2 dibenzo[a,l]pyrene dihydrodiols in mouse skin and rat mammary-gland, Carcinogenesis 12 (1991) 1939–1944.
[14] P. Devanesan, F. Ariese, R. Jankowiak, G.J. Small, E.G. Rogan, E.L. Cavalieri, Preparation, isolation, and characterization of dibenzo[a,l]pyrene diol epoxide-deoxyribonucleoside monophosphate adducts by HPLC anf fluorescence line-narrowing spectroscopy, Chem. Res. Toxicol. 12 (1999) 789–795.
[15] J.L. Mumford, D.B. Harris, K. Williams, J.C. Chuang, M. Cooke, Indoor air samplign and mutagenicity studies of emissions from unvented coal combustion, Environ. Sci. Technol. 21 (1987) 308–311.
[16] S.A. Bortolato, J.A. Arancibia, G.M. Escandar, Non-trilinear chromatographic time retention-fluorescence emission data coupled to chemometric algorithms for the simultaneous determination of 10 polycyclic aromatic hydrocarbons in the presence of interferences, Anal. Chem. 81 (2009) 8074–8084.
[17] S.A. Bortolato, J.A. Arancibia, G.M. Escandar, Chemometrics – assisted fluorimetry for the rapid and selective determination of heavy polycyclic aromatic hydrocarbons in contaminated river waters and activated sludges, Environ. Sci. Technol. 45 (2011) 1513–1520.
[18] I.S. Kozin, C. Gooijer, N.H. Velthorst, Direct determiantion of dibenzo[a,l]pyrene in crude extracts of environmental samples by laser-excited Shpol'skii spectroscopy, Anal. Chem. 67 (1995) 1623–1626.
[19] I.S. Kozin, C. Gooijer, M.H. Velthorst, J. Harmsen, R. Wieggers, Direct determination of isomeric polycyclic aromatic hydrocarbons in environmental samples by conventional and laser excited Shpol'skii spectroscopy, Int. J. Env. Anal. Chem. 61 (1995) 285–297.
[20] A.D. Campiglia, S. Yu, H.Y. Wang, Measuring scatter with a cryogenic probe and an ICCD camera: recording absorption spectra in Shpol'skii matrixes and fluorescence quantum yields in glassy solvents, Anal. Chem. 79 (2007) 1682–1689.
[21] A.J. Bystol, A.D. Campiglia, G.D. Gillispie, Laser-induced multidimensional fluorescence spectroscopy in Shpol'skii matrices with a fiber optic probe at liquid helium temperature, Anal. Chem. 73 (2001) 5762–5770.
[22] A.F.T. Moore, F. Barbosa Jr., A.D. Campiglia, Comb. Cryog. fiber Opt. probes Commer. spectrofluorimeters synchronous Fluoresc. Shpol'skii Spectrosc. High. Mol. Weight. Polycycl. Aromat. Hydrocarb. 68 (2014) 14–25.
[23] S. Yu, A.D. Campiglia, Direct determination nof dibenzo[a,l]pyrene and its four dibenzopyrene isomers in water samples by solid-liquid extraction and laser-excited time-resolved Shpol'skii spectroscopy, Anal. Chem. 77 (2005) 1440–1447.
[24] S. Yu, A.D. Campiglia, Laser-excited time-resolved Shpol'skii spectroscopy for the direct analysis of dibenzopyrene isomers in liquid chromatography fractions, Appl. Spectrosc. 58 (2004) 1385–1393.
[25] W.B. Wilson, A.D. Campiglia, Analysis of co-eluted isomers of high-molecular weight polycyclic aromatic hydrocarbons in high performance liquid chromatography fractiosn via solid-phase nanoextraction and time-resolved Shpol'skii spectroscopy, J. Chromatogr. A 1218 (2011) 6922–6929.
[26] W.B. Wilson, A.D. Campiglia, Determination of polycyclic aromatic hydrocarbons with molecular weight 302 in water samples by solid-phase nanoextraction and laser exicted time-resolved Shpol'skii spectroscopy, Analyst 136 (2011) 3366–3374.
[27] H. Wang, A.D. Campiglia, Determination of polycyclic aromatic hydrocarbons in drinking water samples by solid phase nanoextraction and high-performance liquid chromatography, Anal. Chem. 80 (2008) 8202–8209.
[28] H. Wang, A.D. Campiglia, Direct determination of benzo[a]pyrene in water samples by a gold nanoparticle-based solid phase extraction method and laser-excited time-resolved Shpol'skii spectyrometry, Talanta 83 (2010) 233–240.
[29] H. Wang, S. Yu, A.D. Campiglia, Solid-phase nanoextraction and laser-excited time-resolved Shpol'skii spectroscopy for the analysis of polycyclic aromatic hydrocarbons in drinking water samples, Anal. Biochem. 385 (2009) 249–256.
[30] W.B. Wilson, U. Hewitt, M. Miller, A.D. Campiglia, Water analysis of the sixteen envirionmental protection agency – polycyclic aromatic hydrocarbons via solid-phase nanoextraction-gas chromatography/mass spectrometry, J. Chromatogr. A 1345 (2014) 1–8.
[31] H. Wang, W.B. Wilson, A.D. Campiglia, Using gold nanoparticles to improve the recovery and the limits of dection for the analysis of monohydroxy – polycyclic aromatic hydrocarbons in urine samples, J. Chromatogr. A 1216 (2009) 5793–5799.
[32] H. Wang, G. Knobel, W.B. Wilson, K. Calimag-Williams, A.D. Campiglia, Gold nanoparticles deposited capillaries for in-capillary microextraction capillary zone electrophoresis of monohydroxy – polycyclic aromatic hydrocarbons, Electrophoresis 32 (2011) 720–727.
[33] S.A. Wise, B.A. Benner Jr., G.D. Byrd, S.N. Chesler, R.E. Rebbert, M.M. Schantz, Determiantion of polycyclic aroamtic hydrocarbons in a coal tar standard reference material, Anal. Chem. 60 (1988) 887–894.
[34] A.J. Bystol, T. Thorstenson, A.D. Campiglia, Laser-induced multidimensional fluorescence spectroscopy in Shpol'skii matrices for the analysis of polycyclic aromatic hydrocarbons in HPLC fractions and complex environmental extracts, Environ. Sci. Technol. 36 (2002) 4424–4429.
[35] M.J. Miller, J.C. Miller, Statistics and Chemometrics for Analytical Chemistry, 4th ed., Prentice-Hall, Inc., New York, 2000.
[36] A.C. Olivieri, Practical guidelines for reporting results in single- and multicomponent analytical calibration: a tutorial, Anal. Chim. Acta 868 (2015) 10–22.
[37] A.J. Bystol, S. Yu, A.D. Campiglia, Analysis of polycyclic aromatic hydrocarbons in HPLC fractiosn by laser-excited time-resolved Shpol'skii spectrometry with cryogenic fiber-optic probes, Talanta 60 (2003) 449–458.